









Immiscibility in N₂-H₂O solids up to 140 GPa

Cite as: J. Chem. Phys. **154**, 234505 (2021); <https://doi.org/10.1063/5.0052315>

Submitted: 30 March 2021 . Accepted: 01 June 2021 . Published Online: 17 June 2021

 Xiao Zhang,  Yu Wang,  Maxim Bykov,  Elena Bykova,  Stella Chariton,  Vitali B. Prakapenka, 
Konstantin Glazyrin,  Alexander F. Goncharov, et al.



View Online



Export Citation



CrossMark

ARTICLES YOU MAY BE INTERESTED IN

[Chemistry under extreme conditions: Pressure evolution of chemical bonding and structure in dense solids](#)

Matter and Radiation at Extremes **5**, 018202 (2020); <https://doi.org/10.1063/1.5127897>

[No observation of lead hydride in the Pb-H system under pressure up to 140 GPa](#)

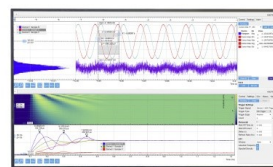
Journal of Applied Physics **129**, 225901 (2021); <https://doi.org/10.1063/5.0056400>

[Internal resistive heating of non-metallic samples to 3000#K and >60#GPa in the diamond anvil cell](#)

Review of Scientific Instruments **92**, 063904 (2021); <https://doi.org/10.1063/5.0038917>

Challenge us.

What are your needs for
periodic signal detection?



Zurich
Instruments



Immiscibility in N₂-H₂O solids up to 140 GPa

Cite as: J. Chem. Phys. 154, 234505 (2021); doi: 10.1063/5.0052315

Submitted: 30 March 2021 • Accepted: 1 June 2021 •

Published Online: 17 June 2021



Xiao Zhang,^{1,2} Yu Wang,¹ Maxim Bykov,³ Elena Bykova,³ Stella Chariton,⁴
Vitali B. Prakapenka,⁴ Konstantin Glazyrin,⁵ and Alexander F. Goncharov^{3,a)}

AFFILIATIONS

¹ Key Laboratory of Materials Physics, Institute of Solid State Physics, HFIPS, Chinese Academy of Sciences, Hefei 230031, Anhui, People's Republic of China

² University of Science and Technology of China, Hefei 230026, China

³ Earth and Planets Laboratory, Carnegie Institution of Washington, 5251 Broad Branch Road NW, Washington, DC 20015, USA

⁴ Center for Advanced Radiation Sources, University of Chicago, Chicago, Illinois 60637, USA

⁵ Deutsches Elektronen-Synchrotron, Notkestrasse 85, 22607 Hamburg, Germany

^{a)} Author to whom correspondence should be addressed: agoncharov@carnegiescience.edu

ABSTRACT

Nitrogen and water are very abundant in nature; however, the way they chemically react at extreme pressure–temperature conditions is unknown. Below 6 GPa, they have been reported to form clathrate compounds. Here, we present Raman spectroscopy and x-ray diffraction studies in the H₂O–N₂ system at high pressures up to 140 GPa. We find that clathrates, which form locally in our diamond cell experiments above 0.3 GPa, transform into a fine grained state above 6 GPa, while there is no sign of formation of mixed compounds. We point out size effects in fine grained crystallites, which result in peculiar Raman spectra in the molecular regime, but x-ray diffraction shows no additional phase or deviation from the bulk behavior of familiar solid phases. Moreover, we find no sign of ice doping by nitrogen, even in the regimes of stability of nonmolecular nitrogen.

Published under an exclusive license by AIP Publishing. <https://doi.org/10.1063/5.0052315>

INTRODUCTION

Water forms numerous inclusion compounds with many elements and molecules. Many of them are clathrate hydrates, where water molecules form cages—hosts incorporating other entities—guests.¹ The structure and composition of these compounds and even their existence depend on the balance between the strength of hydrogen bonds and water–guest interactions,^{2,3} which vary depending on the properties of guest elements or molecules. Under pressure, these open structures modify in such a way that clathrates with large cavities usually collapse and various kinds of filled ices form.^{4–6} Such inclusion compounds have been reported at very high pressures for a number of guests, including Ar, CH₄, H₂, and He.⁶ Understanding of the stability, structure, and properties of these materials is important for various applications, such as gas storage and separation and energy storage, and technological applications, such as cooling devices. Moreover, based on their pressure–temperature (P–T) stability range, these inclusion compounds can be present in interiors of large satellites and planets.^{7,8}

Water can also be considered as a simplest and most familiar hydride which, under pressure, experiences symmetrization of hydrogen bonds and transforms into an extended insulating phase with covalent bonding (ice X) (e.g., Ref. 9). This state is similar to high-pressure phases of other hydrides, H₂S and H₃S, which have been recently examined for high-temperature superconducting properties^{10–13} following the line proposed by Ashcroft for hydrogen dominant alloys.¹⁴ Because these materials comprise light elements, they may have high phonon frequencies and a high density of electronic states, which are necessary ingredients for high-temperature superconductivity. Recently, poly- and super-hydrides have been shown to demonstrate superconductivity close to room temperature,^{10,11} calling for better understanding of their peculiar electronic properties and lattice dynamics which are critical for superconductivity. Water is a natural candidate for detailed examination; however, a dopant is needed to make it metallic as pressure induced doping of water is ineffective.¹⁵ Nitrogen was proposed as a dopant of ice X at 150 GPa¹⁶ substituting oxygen and creating holes as the charge carriers. This material is expected to be a high-temperature superconductor with T_c in the range of 20–60 K.¹⁶

At low pressures, N_2 and H_2O form several host-guest compounds depending on pressure up to 2 GPa.^{3,17–21} Four nitrogen hydrates have been reported below 1.6 GPa; however, the stability of the high-pressure filled ice structure is controversial.⁶ Recently, yet another clathrate structure, $s\text{X}$, with chiral channels of the water molecules has been proposed which are refillable with N_2 molecules.¹⁸ Here, we present combined Raman and synchrotron x-ray diffraction (XRD) investigation of water-nitrogen mixtures in a diamond anvil cell (DAC) up to 140 GPa. We find no sign of nitrogen hydrates above 6 GPa; instead, water and nitrogen followed a common room-temperature sequence of phase transformations. However, the N–N stretching modes demonstrate an unusual splitting in some regions in the DAC cavity where clathrate forms. We assigned these changes in the vibrational spectra to the formation of very small crystallites, causing a violation of the Brillouin zone center Raman selection rules. At high pressures, following the formation of light absorptive amorphous $\eta\text{-N}$, we laser heated the sample up to 3000 K, which resulted in the emergence of familiar polymeric $cg\text{-}$ and $bp\text{-N}$;^{22–25} however, no nitrogen–water compound was documented.

EXPERIMENTAL DETAILS

We performed the experiments in a DAC by combining visual observation with *in situ* high-pressure x-ray diffraction (XRD) and Raman measurements of mixed water–nitrogen samples. The diamond anvils with culets of 500, 300, 200, and 100 μm in diameter (the latter were beveled to 300 μm) were used in experiments up to 140 GPa. Distilled water was put into the cavity drilled in a rhenium gasket, and an air bubble was created in a sealed cavity; then, the DAC was put in a large high-pressure vessel and compressed to 0.15 GPa. N_2 gas was loaded by shortly opening and closing the cavity. Depending on the experimental circumstances, there was an excess of nitrogen or water in the sample cavity, which did not affect the major results. Pressure was measured by using ruby fluorescence, XRD of Au sensors, and Raman spectroscopy of the stressed anvils depending on the experiment type and availability. All the measurements and pressure manipulations have been performed at room temperature. Near infrared fiber laser heating (1064 nm) was attempted at several pressures above 10 GPa via a direct coupling scheme, but no sizable effects have been observed visually and by Raman spectroscopy. In addition, to address possible kinetic effects on the formation of clathrate compounds, we performed laser heating above the melt line of ice VII and N_2 at about 10 GPa by coupling the laser beam to small Au pieces in the high-pressure cavity. Above 130 GPa, we directly laser heated the sample following the appearance of amorphous $\eta\text{-N}$,^{26,27} which absorbs laser radiation, leading to synthesis of polymeric nitrogen modifications.

Of several (~ 10) experiments that have been performed, the majority were visual/Raman, while three combining visual observations with concomitant synchrotron x-ray diffraction (XRD)/Raman investigations were performed at GSECARS (Sector 13 of the Advanced Photon Source, the Argonne National Laboratory) and the Extreme Conditions Beamline (ECB) P02.2 (Petra III, Deutsches Elektronen-Synchrotron, Hamburg, Germany). Our confocal Raman probe at the Institute of Solid State Physics (Hefei, China) utilizes any of the 488, 532, and 660 nm laser excitation

wavelengths.²⁸ The Raman notch filters allow Raman measurements down to 10 cm^{-1} in the Stokes and anti-Stokes spectral ranges. One of these notch filters is used as a beamsplitter to inject the laser beam into the optical path. A single stage imaging spectrograph SP2500 (Acton) with a focal length of 500 mm was equipped with an array thermoelectrically cooled CCD detector (Princeton eXcelon). Normally, spectra were acquired in a low resolution mode (300 grooves/mm grating) for a quick reconnaissance followed by a longer time ($<300\text{ s}$) acquisition using a high spectral resolution mode (1200 or 1800 grooves/mm grating), yielding approximately a spectral resolution of 4 cm^{-1} . The laser power was limited to values below 20 mW at the sample to avoid sample overheating. The offline Raman system at GSECARS has a similar optical schematic.²⁹ The latter system has mapping capabilities, which were extensively used for investigations of heterogeneous samples investigated here.

Synchrotron XRD experiments were performed at GSECARS with the wavelength of 0.2952 Å and ECB with the wavelength of 0.291 Å by employing both powder and single-crystal techniques. In the latter case, we collected XRD patterns at different angular positions of a DAC with respect to the ω rotation axis (vertical) with the samples carefully positioned on the rotation center (e.g., Ref. 30). XRD mapping capabilities were also extensively employed, and the Raman and XRD maps were analyzed together. The x-ray beam size was $\sim 3 \times 3\text{ }\mu\text{m}^2$ at GSECARS and $\sim 2 \times 2\text{ }\mu\text{m}^2$ at ECB.

RESULTS AND DISCUSSIONS

After loading, while at low pressures, fluid H_2O and N_2 were spatially separated with N_2 filling spherical-like vesicles based on visual observations and Raman measurements (Figs. 1 and 2 and Fig. S1 of the supplementary material). Judging from very low intensity of the N–N stretching mode (vibron) at 2330 cm^{-1} in the Raman spectra of the water-rich sample, the solubility of N_2 in water is very low, and this situation remains after ice forms at about 2 GPa (Fig. 1). The nitrogen-rich part of the sample

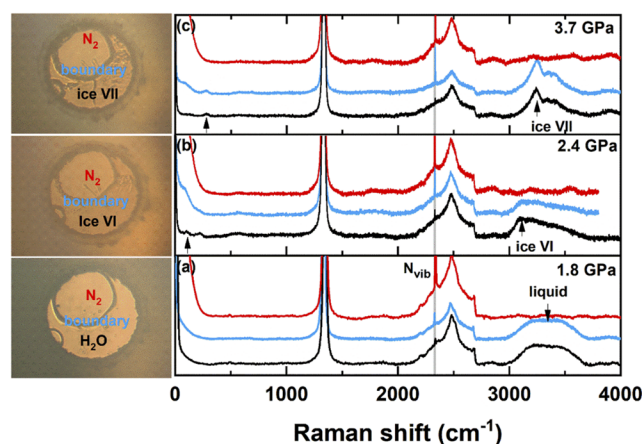


FIG. 1. Raman spectra of different regions of samples and corresponding microscopic images of $\text{N}_2\text{-H}_2\text{O}$ at elevating pressures. The light gray solid line is a guide to the eye for comparing the frequency of the N_2 vibron at different sample locations. Panels (a)–(c) correspond to various pressures.

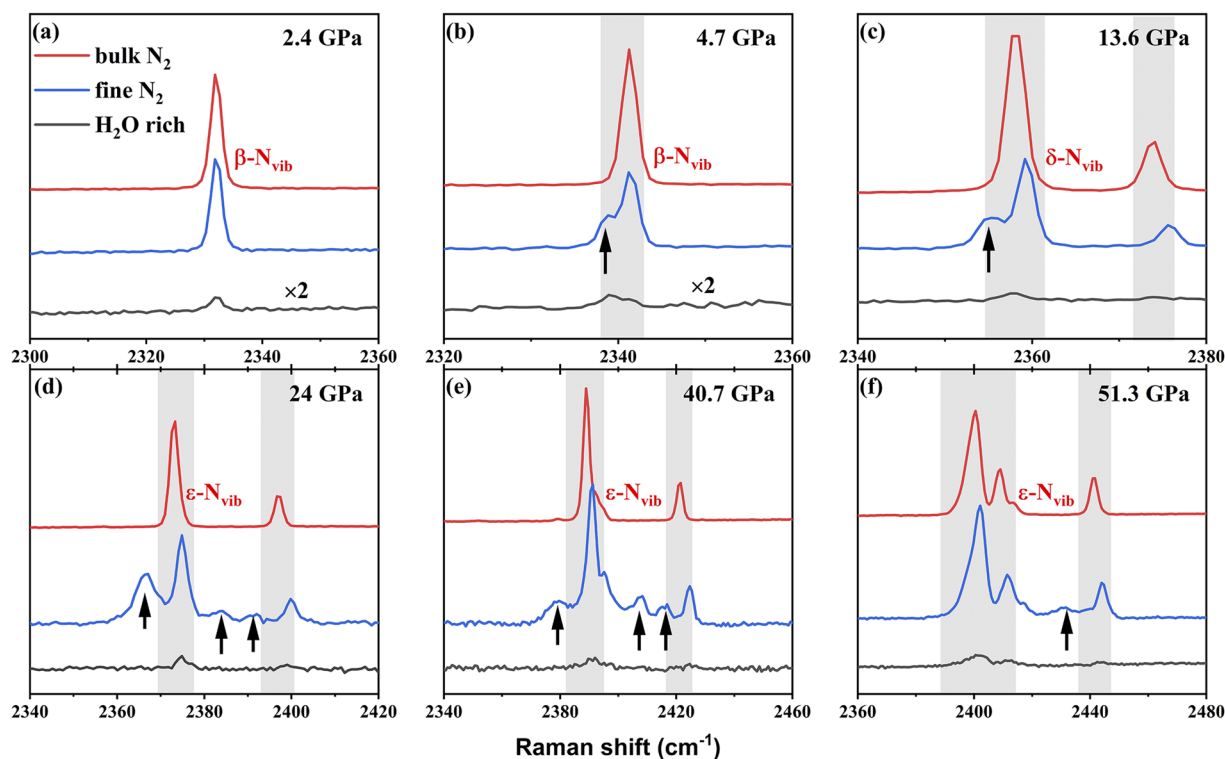


FIG. 2. Raman spectra of the N–N vibron in the water-rich sample (in dark gray), in bulk N₂ (in red), and in mixed N₂–H₂O (in blue) at different pressures. The arrows mark additional Raman peaks that appear in heavily mixed sample areas. The light gray boxes are guides to the eye for easy comparison of the mode frequencies. Panels (a)–(f) correspond to various pressures.

shows no sign of the O–H stretch modes at 3200–3500 cm^{−1}. The Raman spectra of the water- and N₂-rich areas could not be distinguished from those of the bulk materials, the high-pressure behavior of which had been described previously.^{9,26,31} Their Raman frequencies agree well with the literature data as shown in Fig. 3. Upon an increase in pressure, the boundaries between water- and N₂-rich areas become fuzzier, but they remain visible to very high pressures.

Clathrates reported previously have been detected in a number of experiments via observations of a splitting of the intramolecular N–N vibration (vibron) at about 1 GPa (Fig. 3)^{19,20} and by concomitant visual observations. Depending on the initial water–nitrogen composition in the cavity, clathrates form in boundary regions between H₂O- and N₂-rich zones or the sample is split between the clathrate and H₂O- or N₂-rich regions (Fig. S2 of the [supplementary material](#)). However, upon an increase in pressure, the Raman spectra of the regions originating from clathrates and supposedly phase separated demonstrate somewhat modified Raman spectra; we attribute these characteristics to a fine grained mixture of solid N₂ and H₂O as discussed below.

We examined the stability of fine grained mixtures by laser heating at 10 GPa deposited via Au pieces positioned in the proximity to the sample. In this experiment, H₂O–N₂ sample including the fine grained region (Fig. S2 of the [supplementary material](#)) was melted around laser heated Au pieces. Visual observations

demonstrated no essential change in the sample appearance, while Raman measurements showed a splitting of the ν_2 mode (Fig. S3 of the [supplementary material](#)), the effect which we associate with the presence of very small crystallites as discussed below. There was no further time dependent change following these observations over several hours.

At 4.7 GPa, the N₂ vibron mode shows a splitting (Fig. 2) in the fine grained region and a new broad peak that appears at lower frequencies, while bulk N₂ (β -phase) reveals only one vibron peak at this pressure.³² At higher pressures, in the stability region of δ and ϵ phases, where the vibron modes split into ν_1 and ν_2 vibron components due to the presence of two nonequivalent crystallographic sites, this splitting persists for the lower frequency ν_2 vibron component, while the ν_1 mode remains a single component. The intensity of the new Raman peak and the splitting value are critically dependent on the sample positions (Figs. S1 and S4 of the [supplementary material](#)).

Above 20 GPa, two new Raman peaks appear between the ν_1 and ν_2 major vibron components in addition to a common splitting of the ν_2 mode, which occurs in ϵ -N₂.³³ Above 42 GPa, the lower frequency component of the ν_2 vibron gets weaker [Fig. 2(e)], while the main ν_2 peak becomes asymmetric (Fig. 2 and Fig. S1 of the [supplementary material](#)). The results of two experiments, where the additional peaks were observed, slightly vary in terms of the frequencies and the peak intensities depending on the sample

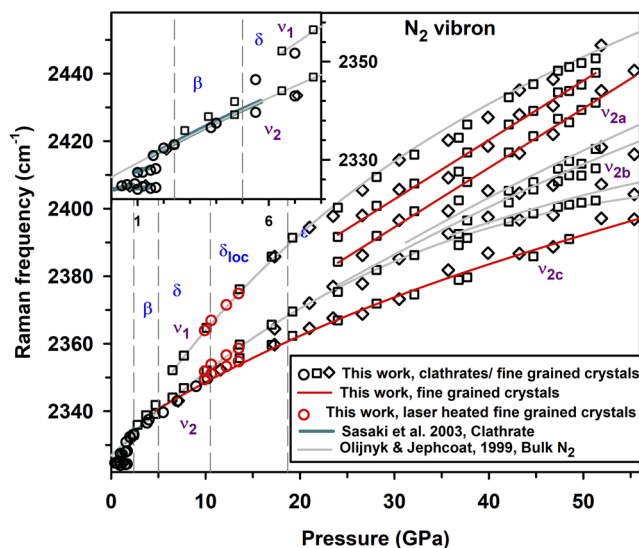


FIG. 3. Pressure dependencies of the Raman vibron frequencies of fine grained N_2 (black open symbols) in comparison with bulk N_2 (gray solid lines, Ref. 31). The red solid lines are guides to the eye, emphasizing the additional Raman bands of fine grained N_2 . The inset shows the detailed low-pressure behavior, in agreement with the data of Refs. 19 and 20 (dark cyan solid lines), which assigned the observed peaks to the NH-II clathrate.

positions; this suggests that these observations in highly heterogeneous N_2 - H_2O mixtures may be related to crystal habit and/or size effects. The vibrational frequencies of the v_1 and v_2 major vibron modes of fine grained N_2 agree well with those of bulk N_2 (Fig. 3). It is interesting that similar spectra were also observed in the water-rich area of the sample, where the additional vibron peaks are stronger (Fig. S4 of the [supplementary material](#)).

The lattice modes measured in the fine grained area generally show a good correspondence with those of bulk nitrogen (Fig. S1 of the [supplementary material](#)). The ice VII lattice mode is observed below 22 GPa (Fig. S4 of the [supplementary material](#)), but at higher pressures, narrow and strong lattices of ϵ - N_2 dominate in the spectrum. The O-H stretching and bending modes also show a good correspondence with the behavior of bulk ice VII (Fig. S5 of the [supplementary material](#)).

Above 87 GPa, in the stability range of the ζ phase of N_2 ,^{34,35} the v_1 vibron mode in the fine grained area demonstrates a departure from bulk N_2 to higher frequencies, while the v_2 modes show a good correspondence (Fig. S6 of the [supplementary material](#)). Moreover, the v_1 vibron mode persists and remains strong up to at least 132 GPa in contrast to bulk nitrogen, where this mode becomes very weak, which is likely related to the transformation to κ - N_2 .³⁴ The departure of the v_1 vibron mode to higher frequencies has been also observed in the He- N_2 system, where the $(N_2)_{11}$ He compound was reported to be stable up to 135 GPa in a structure similar to ϵ - N_2 .³⁶ As in the case of the anomalous N_2 vibron peaks at lower pressures, the blue-shifted v_1 Raman vibron was also observed in the water-rich area of the sample, where it was relatively stronger (Fig. S7 of the [supplementary material](#)). It is worth noting that the frequency of the T_{2g} O-O stretch mode of ice X measured of the same fine grained

area is consistent with that measured from the bulk material⁹ (Fig. S8 of the [supplementary material](#)).

The frequency of the vibron mode depends on the molecular environment and intermolecular coupling. The latter term strongly depends on whether the crystallites are sufficiently large, so their inverse length value is smaller than the wave vector of the vibrational excitations. The Raman selection rules, which dictate that only the Brillouin zone center modes are allowed due to the conservation of momentum, fail in this limit. As a result, the vibron impurity modes appear with the frequencies of non-interacting molecules, which are substantially different from that in the bulk crystal.³⁷ This mechanism provides a tentative explanation to an unusual behavior of N_2 vibron modes (Figs. 2 and 3), suggesting that it is the size effect, which results in observations of extra Raman peaks in the vibrational spectra of nanocrystallites.

X-ray diffraction measurements have been performed on several N_2 - H_2O samples above 6 GPa up to 140 GPa. The experiments involved collection of powder diffraction in an area of interest using grid scans with a typical step size of 2 μ m and covering the range of $\pm 15 \mu$ m relative to the center of the sample chamber or the region of interest [Figs. 4(a)–4(c) and Fig. S9 of the [supplementary material](#)]. The sample contained clearly distinct H_2O - and N_2 -rich areas. Both H_2O and N_2 crystallize in the structures typical for the pure systems at given pressures. At ~ 7 GPa, N_2 possesses a cubic $Pm\bar{3}n$ structure (δ - N_2) with $a = 5.9656(9)$ Å [Fig. 4(a)], while water crystallizes in the ice-VII structure ($Pn\bar{3}m$) with $a = 3.1866(4)$ Å. The unit cell volumes measured here for various nitrogen and ice phases are in agreement with the previous observations (Fig. 5). Due to the *bcc* arrangement of oxygen atoms in the unit cell of ice-VII, the reflections (*hkl*) with $h + k + l = 2n + 1$ have negligible intensities and were not used for the Le-Bail fit to avoid ambiguities resulting from possible overlaps between these reflections and the reflections of δ - N_2 .

On further compression, nitrogen transforms to the ϵ - N_2 phase [Fig. 4(b)], while H_2O can no longer be described very well by a cubic symmetry: the cubic lattice parameter deduced from the position of reflections (110) and (002) deviates by ~ 0.015 Å, suggesting either the symmetry lowering or the development of non-hydrostatic stress conditions (Table S1 of the [supplementary material](#)). This effect was previously observed by Somayazulu *et al.*³⁸ Quasi-continuous rings of ϵ - N_2 are observed in H_2O -rich areas where nitrogen forms very small crystallites consistently with observations of extra Raman vibron peaks (Fig. S9 of the [supplementary material](#)).

We found no evidence of crystalline mixed N_2 - H_2O compounds up to the highest pressure reached in this study even when the sample was heated. Above 120 GPa, molecular nitrogen can be transformed to nonmolecular η -N via direct laser heating.^{25,34,39} This results in the formation of *cg*-N and *bp*-N (at slightly higher pressures), in agreement with previous studies^{23–25,34,39,40} [Fig. 4(c), Fig. 5].

Previous studies suggested that filled ice structures (FIS) form in the H_2O - N_2 system and remain stable to high pressures, at least 6 GPa,²⁰ perhaps to 30 GPa.⁶ However, the structure was only reported below 2 GPa and no structural refinement was presented,³ while the vibrational spectroscopy data are too ambiguous to claim the stability of FIS to higher pressures. Raman spectroscopy data of this work are consistent with the presence of the well-known phases of ice and nitrogen, while the extra N_2 vibron and lattice mode peaks are likely due to the size effects (Figs. 1–3 and Figs. S1, S3, S5, and S6

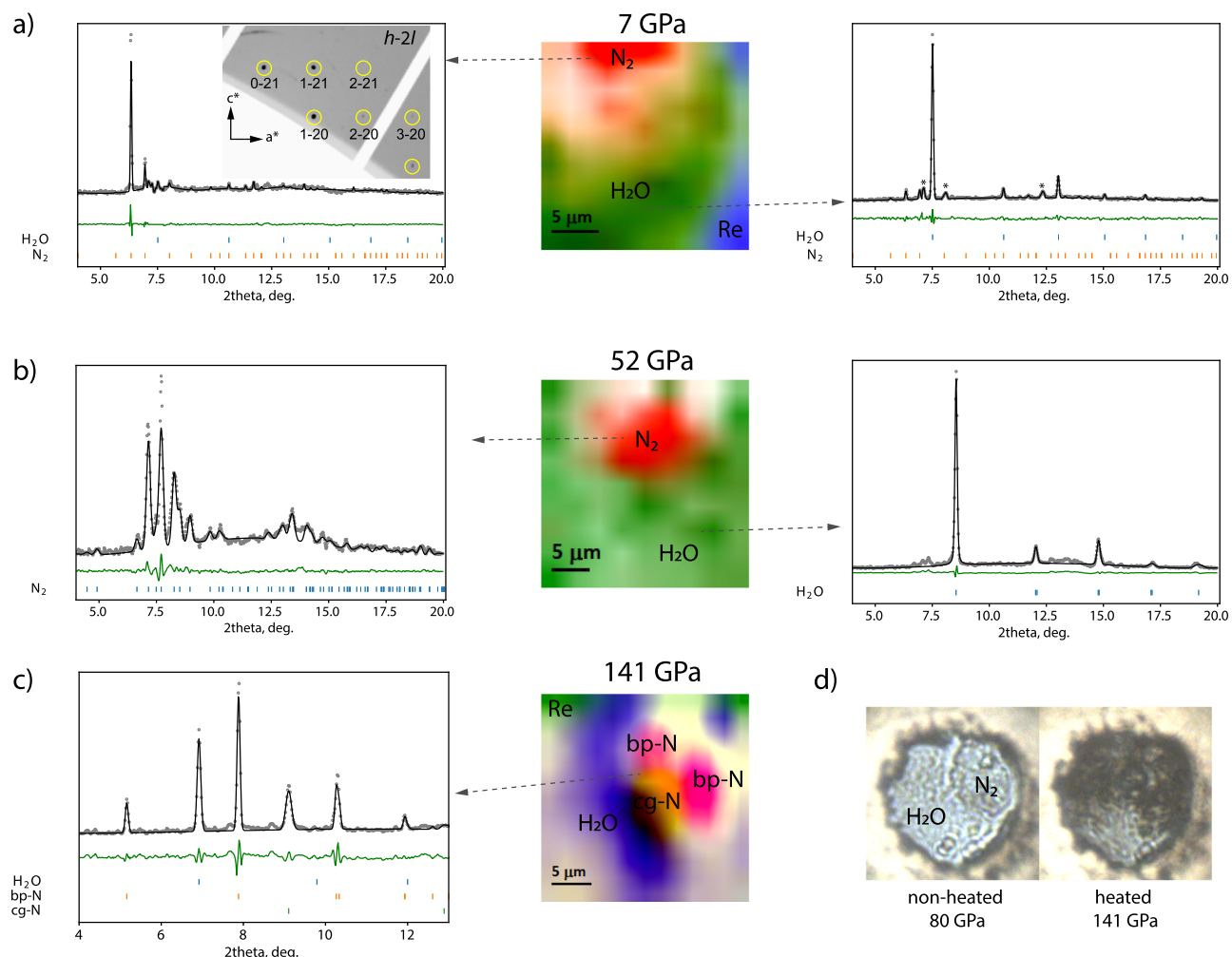


FIG. 4. (a)–(c) X-ray diffraction imaging maps of the N₂–H₂O sample at various pressures and representative powder diffraction patterns $\lambda = 0.2952 \text{ \AA}$. (d) Microscopic images of non-heated and heated N₂–H₂O samples at various pressures.

of the [supplementary material](#)). A splitting of the N₂ vibron mode above 5 GPa indicates the transition into a common δ -phase of bulk nitrogen. The structure and lattice parameters of the detected solid nitrogen phases are verified by direct single-crystal and powder XRD measurements [Fig. 4(a), Fig. (5)]. Moreover, the presence of ice VII has also been documented, while no other phase was found. These results demonstrate the instability of FIS phases with respect to decomposition to end-member materials. This is in contrast to other mixed molecular systems, such as H₂–H₂O and CH₄–H₂O, where inclusion compounds are stable at very high pressures.^{4,5,41} Following Ref. 3, N₂ hydrate has an orthorhombic Methane Hydrate III (MH-III) structure⁴² at 2 GPa with a N₂ to H₂O ratio of 2:1, yielding a volume of some 4% larger than the mean volume of the β -N₂ and ice VII mixture at a ratio of 2:1, while isostructural CH₄–H₂O is as dense as the mixture. This loose packing of N₂–H₂O FIS indicates that it is prompt to instability with regard to dissociation, and this tendency likely increases with pressure as N₂ is very compressible,

and it is more compressible than methane at 2–15 GPa (Fig. S10 of the [supplementary material](#)).

Doping of ice X has been examined theoretically at 150 GPa to explore a possibility to close the bandgap and create a new high-temperature superconducting hydride.¹⁶ Our experiments do show that the samples become absorptive at above 140 GPa, but this must be due to transition into amorphous η -N.^{26,27} After laser heating at 140 GPa up to 3000 K, *cg*- and *bp*-N formed in the cavity; however, the sample remains dark in the nitrogen-rich part [Fig. 4(c)]. This seems to be in odd with the reported transparency of both *cg*- and *bp*-N.^{23–25} Indeed, the dark parts of the sample contain a substantial amount of *bp*-N manifested by the strong characteristic Raman spectra (Fig. S11 of the [supplementary material](#)). The sample was coupling to an IR heating laser after several heating events up to the highest temperatures. We could even laser heat the sample at 80–84 GPa following the pressure release from 140 GPa, suggesting that *bp*-N can be absorptive (cf. Refs. 23 and 24) in this pressure

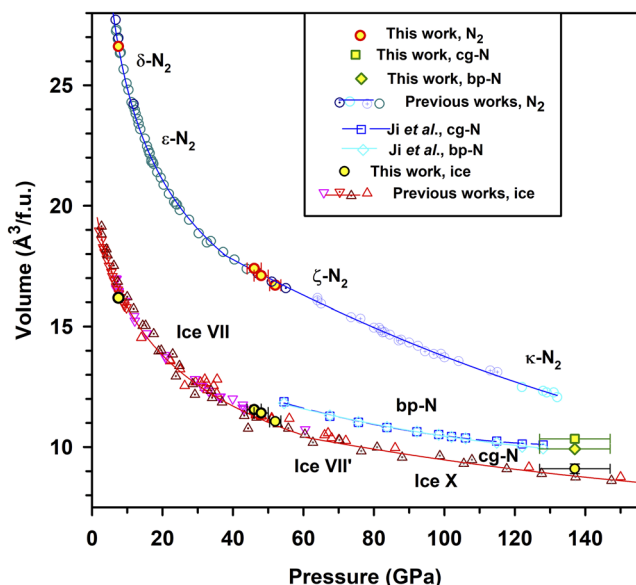


FIG. 5. Volume per formula unit vs pressure of solid phases of nitrogen (per two atoms for polymeric phases) and water. The error bars are smaller than the symbol size (not shown). The results of the previous works on nitrogen are from Refs. 23, 24, 34, 43, and 44 and on ice are from Refs. 45–48.

range. In addition to these phases, we could even detect patches of molecular nitrogen owing to the observations of N_2 vibron modes at 2378 cm^{-1} and a few weaker higher frequency bands (Fig. S11 of the [supplementary material](#)). The T_{2g} oxygen mode of the symmetric ice X phase⁹ is broad and weak and could be occasionally observed (Figs. S7 and S11 of the [supplementary material](#)). We can speculate that the interphase boundaries contribute to the absorption processes even though XRD and Raman spectroscopy measurements do not reveal any other signals but those which can be attributed to the major nitrogen and water phases described above. These include Raman modes η -, cg -, and bp - N ,^{23–27} as well ice X (Fig. S11 of the [supplementary material](#)). The spectral positions of all the Raman bands agree well with those of the bulk materials at the same pressure (Fig. S8 of the [supplementary material](#)).

CONCLUSIONS

Our combined XRD and Raman experiments above 6 GPa show no sign of stability for filled ice structures, unlike the case of the reportedly structurally similar CH_4 – H_2O system, which is stable at very high pressures. However, the existence of filled ice structures cannot be completely ruled out unless other P-T pathways and longer synthesis times are explored. Nevertheless, we find a remarkable immiscibility of common stable phases of nitrogen in both the molecular and nonmolecular regimes. The additional nitrogen originated Raman bands which have been observed in heavily mixed H_2O and N_2 sample regions were assigned to the crystallite size effects due to the breakdown of the Raman selection rules. A detailed XRD mapping of mixed samples before and after laser heating up to 3000 K at 140 GPa demonstrated no effect of ice doping by nitrogen. A dark appearance of the

mixed samples at high pressures is likely due to combined effects of fine grain boundaries and the presence of nonmolecular forms of nitrogen.

AUTHORS' CONTRIBUTIONS

X.Z. and Y.W. contributed equally to this work.

SUPPLEMENTARY MATERIAL

See the [supplementary material](#) for 11 figures and one table.

ACKNOWLEDGMENTS

This work was supported by the National Natural Science Foundation of China (Grant Nos. 51672279, 51727806, 11874361, and 11774354), the CASHIPS Director's Fund (Grant Nos. YZJJ201705 and YZJJ2020QN22), and Science Challenge Projects (Nos. TZ2016001 and TZ2016001). Part of this work was performed at GeoSoilEnviroCARS (The University of Chicago, Sector 13), the Advanced Photon Source (APS), and Argonne National Laboratory. GeoSoilEnviroCARS is supported by the National Science Foundation—Earth Sciences (Grant No. EAR-1634415). The Advanced Photon Source is a U.S. Department of Energy (DOE) Office of Science user facility operated for the DOE Office of Science by Argonne National Laboratory under Contract No. DE-AC02-06CH11357. The use of the GSECARS Raman Lab System was supported by the NSF MRI Proposal (No. EAR-1531583). Part of this research was carried out at the Extreme Conditions Beamline (P02.2) at the DESY, a member of Helmholtz Association (HGF). M.B., E.B., and A.F.G. acknowledge the support of the Carnegie Institution of Washington.

DATA AVAILABILITY

The data that support the findings of this study are available within the article and its [supplementary material](#).

REFERENCES

- 1 J. E. Dendy Sloan and C. A. Koh, *Chemical Industries Series*, 3rd ed. (CRC Press, 2007).
- 2 J. S. Tse, M. L. Klein, and I. R. McDonald, *J. Phys. Chem.* **87**(21), 4198–4203 (1983).
- 3 J. S. Loveday, R. J. Nelmes, D. D. Klug, J. S. Tse, and S. Desgreniers, *Can. J. Phys.* **81**(1–2), 539–544 (2003).
- 4 S.-i. Machida, H. Hirai, T. Kawamura, Y. Yamamoto, and T. Yagi, *Phys. Earth Planet. Inter.* **155**(1–2), 170–176 (2006).
- 5 W. L. Vos, L. W. Finger, R. J. Hemley, and H.-k. Mao, *Phys. Rev. Lett.* **71**(19), 3150–3153 (1993).
- 6 J. S. Loveday and R. J. Nelmes, *Phys. Chem. Chem. Phys.* **10**(7), 937–950 (2008).
- 7 J. I. Lunine and D. J. Stevenson, *Icarus* **70**(1), 61–77 (1987).
- 8 J. S. Loveday, R. J. Nelmes, M. Guthrie, S. A. Belmonte, D. R. Allan, D. D. Klug, J. S. Tse, and Y. P. Handa, *Nature* **410**(6829), 661–663 (2001).
- 9 A. F. Goncharov, V. V. Struzhkin, H.-k. Mao, and R. J. Hemley, *Phys. Rev. Lett.* **83**(10), 1998–2001 (1999).
- 10 A. P. Drozdov, M. I. Erements, I. A. Troyan, V. Ksenofontov, and S. I. Shylin, *Nature* **525**(7567), 73–76 (2015).
- 11 E. Snider, N. Dasenbrock-Gammon, R. McBride, M. Debessai, H. Vindana, K. Vencatasamy, K. V. Lawler, A. Salamat, and R. P. Dias, *Nature* **586**(7829), 373–377 (2020).

- ¹²D. Duan, Y. Liu, F. Tian, D. Li, X. Huang, Z. Zhao, H. Yu, B. Liu, W. Tian, and T. Cui, *Sci. Rep.* **4**, 6968 (2014).
- ¹³Y. Li, J. Hao, H. Liu, Y. Li, and Y. Ma, *J. Chem. Phys.* **140**(17), 174712 (2014).
- ¹⁴N. W. Ashcroft, *Phys. Rev. Lett.* **92**(18), 187002 (2004).
- ¹⁵C. J. Pickard, M. Martinez-Canales, and R. J. Needs, *Phys. Rev. Lett.* **110**(24), 245701 (2013).
- ¹⁶J. A. Flores-Livas, A. Sanna, M. Gražinytė, A. Davydov, S. Goedecker, and M. A. L. Marques, *Sci. Rep.* **7**(1), 6825 (2017).
- ¹⁷Y. A. Dyadin, E. G. Larionov, E. Y. Aladko, and F. V. Zhurko, *Dokl. Phys. Chem.* **378**(4), 159–161 (2001).
- ¹⁸B. Massani, L. J. Conway, A. Hermann, and J. Loveday, *J. Chem. Phys.* **151**(10), 104305 (2019).
- ¹⁹M. G. E. van Hinsberg, M. I. M. Scheerboom, and J. A. Schouten, *J. Chem. Phys.* **99**(1), 752–754 (1993).
- ²⁰S. Sasaki, S. Hori, T. Kume, and H. Shimizu, *J. Chem. Phys.* **118**(17), 7892–7897 (2003).
- ²¹C. Petuya, F. Damay, B. Chazallon, J.-L. Bruneel, and A. Desmedt, *J. Phys. Chem. C* **122**(1), 566–573 (2018).
- ²²C. Mailhot, L. H. Yang, and A. K. McMahan, *Phys. Rev. B* **46**(22), 14419–14435 (1992).
- ²³D. Laniel, B. Winkler, T. Fedotenko, A. Pakhomova, S. Chariton, V. Milman, V. Prakapenka, L. Dubrovinsky, and N. Dubrovinskaia, *Phys. Rev. Lett.* **124**(21), 216001 (2020).
- ²⁴C. Ji, A. A. Adeleke, L. Yang, B. Wan, H. Gou, Y. Yao, B. Li, Y. Meng, J. S. Smith, V. B. Prakapenka, W. Liu, G. Shen, W. L. Mao, and H.-k. Mao, *Sci. Adv.* **6**(23), eaba9206 (2020).
- ²⁵M. I. Eremets, A. G. Gavriliuk, I. A. Trojan, D. A. Dzivenko, and R. Boehler, *Nat. Mater.* **3**(8), 558–563 (2004).
- ²⁶A. F. Goncharov, E. Gregoryanz, H.-k. Mao, Z. Liu, and R. J. Hemley, *Phys. Rev. Lett.* **85**(6), 1262–1265 (2000).
- ²⁷E. Gregoryanz, A. F. Goncharov, R. J. Hemley, and H.-k. Mao, *Phys. Rev. B* **64**(5), 052103 (2001).
- ²⁸A. F. Goncharov, N. Holtgrewe, G. Qian, C. Hu, A. R. Oganov, M. Somayazulu, E. Stavrou, C. J. Pickard, A. Berlie, F. Yen, M. Mahmood, S. S. Lobanov, Z. Konôpková, and V. B. Prakapenka, *J. Chem. Phys.* **142**(21), 214308 (2015).
- ²⁹N. Holtgrewe, E. Greenberg, C. Prescher, V. B. Prakapenka, and A. F. Goncharov, *High Pressure Res.* **39**(3), 457–470 (2019).
- ³⁰A. F. Goncharov, M. Bykov, E. Bykova, K. Glazyrin, V. Prakapenka, Z.-Y. Cao, and X.-J. Chen, *Phys. Rev. B* **102**(6), 064105 (2020).
- ³¹H. Olijnyk and A. P. Jephcoat, *Phys. Rev. Lett.* **83**(2), 332–335 (1999).
- ³²S. Buchsbaum, R. L. Mills, and D. Schiferl, *J. Phys. Chem.* **88**(12), 2522–2525 (1984).
- ³³D. Schiferl, S. Buchsbaum, and R. L. Mills, *J. Phys. Chem.* **89**(11), 2324–2330 (1985).
- ³⁴E. Gregoryanz, A. F. Goncharov, C. Sanloup, M. Somayazulu, H.-k. Mao, and R. J. Hemley, *J. Chem. Phys.* **126**(18), 184505 (2007).
- ³⁵R. Bini, L. Ulivi, J. Kreutz, and H. J. Jodl, *J. Chem. Phys.* **112**(19), 8522–8529 (2000).
- ³⁶S. Ninet, G. Weck, P. Loubeyre, and F. Datchi, *Phys. Rev. B* **83**(13), 134107 (2011).
- ³⁷P. Loubeyre, R. LeToullec, and J. P. Pinceaux, *Phys. Rev. B* **45**, 12844 (1992).
- ³⁸M. Somayazulu, J. Shu, C.-s. Zha, A. F. Goncharov, O. Tschauner, H.-k. Mao, and R. J. Hemley, *J. Chem. Phys.* **128**(6), 064510 (2008).
- ³⁹M. J. Lipp, J. P. Klepeis, B. J. Baer, H. Cynn, W. J. Evans, V. Iota, and C. S. Yoo, *Phys. Rev. B* **76**(1), 014113 (2007).
- ⁴⁰P. Cheng, X. Yang, X. Zhang, Y. Wang, S. Jiang, and A. F. Goncharov, *J. Chem. Phys.* **152**(24), 244502 (2020).
- ⁴¹H. Hirai, T. Tanaka, T. Kawamura, Y. Yamamoto, and T. Yagi, *J. Phys. Chem. Solids* **65**(8–9), 1555–1559 (2004).
- ⁴²J. S. Loveday, R. J. Nelmes, M. Guthrie, D. D. Klug, and J. S. Tse, *Phys. Rev. Lett.* **87**(21), 215501 (2001).
- ⁴³R. L. Mills, B. Olinger, and D. T. Cromer, *J. Chem. Phys.* **84**(5), 2837–2845 (1986).
- ⁴⁴H. Olijnyk, *J. Chem. Phys.* **93**(12), 8968–8972 (1990).
- ⁴⁵M. R. Frank, Y. Fei, and J. Hu, *Geochim. Cosmochim. Acta* **68**(13), 2781–2790 (2004).
- ⁴⁶P. Loubeyre, R. LeToullec, E. Wolanin, M. Hanfland, and D. Hausermann, *Nature* **397**(6719), 503–506 (1999).
- ⁴⁷L. Bezacier, B. Journaux, J.-P. Perrillat, H. Cardon, M. Hanfland, and I. Daniel, *J. Chem. Phys.* **141**(10), 104505 (2014).
- ⁴⁸V. B. Prakapenka, N. Holtgrewe, S. S. Lobanov, and A. Goncharov, *arXiv:2007.07715v1* [cond-mat.mtrl-sci] (2020).